JOURNAL OF CANCER PREVENTION
VOL. 18, NO. 3, SEPTEMBER, 2013

pISSN 2288-3649 · eISSN 2288-3657

ORIGINAL ARTICLE

Global Inactivation of the *Pla2g6* Gene in Mice Does Not Cause Dyslipidemia under Chow or High-fat Diet Conditions

Li Zhang[1,*], Shumei Zhong[2,*], Ying Li[3], Guang Ji[1], Meenakshi Sundaram[2], Zemin Yao[2]

[1]Institute of Digestive Disease, Longhua Hospital, Shanghai University of Traditional Chinese Medicine, Shanghai, China, [2]Department of Biochemistry, Microbiology and Immunology, Ottawa Institute of Systems Biology, University of Ottawa, Ottawa, Canada, [3]College of Life Science, Chongqing Normal University, Chongqing, China

Background: Genome-wide association studies suggest that plasma triacylglyceride (TAG) in humans was associated with variation in the *PLA2G6* locus, a gene that encodes calcium-independent phospholipase A_2 (iPLA$_2\beta$). The objective of the present study is to understand the impact of genetic inactivation of iPLA$_2\beta$ on hepatic TAG metabolism in C57BL/6 mice.
Methods: Male iPLA$_2\beta^{+/-}$ mice were backcrossed with female iPLA$_2\beta^{-/-}$ mice for up to 10 generations prior to experiments. Lipid and lipoprotein metabolism from plasma, hepatocytes, thigh subcutaneous adipose and thigh skeletal muscle tissues of the mice were determined under various experimental conditions.
Results: The iPLA$_2\beta^{-/-}$ mice, either male or female as compared with iPLA$_2\beta^{+/+}$ littermates, showed no change in fasted or postprandial plasma TAG or total cholesterol at young (12-15 weeks) or old (40-44 weeks) ages under chow diet or high-fat diet (HFD) conditions. However, fractionation of plasma lipoproteins showed that under HFD conditions, there was a significant increase (by 40%) in apoB-100 association with $VLDL_1$ fractions in iPLA$_2\beta^{-/-}$ mice as compared with iPLA$_2\beta^{+/+}$ littermates. There was no significant difference in triglyceride or cholesterol contents in the liver, muscle, or adipose tissue between iPLA$_2\beta^{-/-}$ and iPLA$_2\beta^{+/+}$ littermates. Metabolic labeling experiments with cultured primary hepatocytes isolated from iPLA$_2\beta^{-/-}$ mice also showed 2-fold increase in the secretion of [^{35}S]methionine-labeled apoB-100 in $VLDL_1$ fractions as compared with that from iPLA$_2\beta^{+/+}$ hepatocytes. Likewise, secretion of [^{3}H]palmitate-labeled TAG from the iPLA$_2\beta^{-/-}$ hepatocytes was increased by 2-fold.
Conclusions: Although iPLA$_2\beta$ may play a role in TAG-rich $VLDL_1$ production from cultured hepatocytes, there is no evidence that inactivation of iPLA$_2\beta$ would lead to dyslipidemia in mice *in vivo*. (J Cancer Prev 2013;18:235-248)

Key Words: Phospholipase A_2, iPLA$_2\beta$, Triglyceride, Cholesterol, VLDL

INTRODUCTION

The concentration of plasma triacylglycerol (TAG), like that of total cholesterol and low-density lipoprotein (LDL)-associated cholesterol, is considered as a heritable risk factor for cardiovascular diseases.[1] Plasma TAG concentration is influenced by multiple factors including the rate of TAG-rich lipoprotein (e.g. hepatic very-low density lipoproteins and intestinal chylomicrons) production, the rate of TAG-rich lipoprotein catabolism (e.g. hydrolysis catalyzed by hepatic lipases and lipoprotein lipases), and the rate of remnant lipoprotein clearance.[2] Increased *de novo* lipogenesis, excess intake of dietary fatty acids derived from remnant lipoproteins, and elevated influx of fatty acids derived from adipocyte lipolysis, particularly under diabetic and insulin resistance conditions, contribute to overproduction of hepatic TAG-rich lipoproteins and often abnormal accumulation of TAG in the liver

Received August 30, 2013, **Revised** September 10, 2013, **Accepted** September 10, 2013

Correspondence to: Zemin Yao
Department of Biochemistry, Microbiology and Immunology, Ottawa Institute of Systems Biology, University of Ottawa, Ottawa, Ontario K1H 8M5, Canada
Tel: +1-613-562-5800 Ext. 3952, Fax: +1-613-562-5452, E-mail: zyao@uottawa.ca
*The first two authors equally contributed to this work.

(commonly known as non-alcoholic fatty liver disease (NAFLD)).[3]

A recent comprehensive genome-wide association studies reported by the Global Lipids Genetics Consortium have identified known and novel 32 loci harboring common variants that contribute to variations in plasma TAG concentrations, one of the novel loci is the *PLA2G6* locus.[4] The PLA2G6 genes encodes calcium-independent phospholipase A_2 (iPLA$_2\beta$), also known as PNPLA9, an 85-kDa protein that is a member of the patatin-like phospholipase domain-containing lipase family.[5] In addition to the PLA_2 activity, iPLA$_2\beta$ also possess the activities of lysophospholipase, transacylase, and acyl-CoA thioesterase.[6] Many signaling functions have been ascribed to the activity of iPLA$_2\beta$, including regulation of insulin secretion, cell activation, proliferation, migration, and apoptosis.[7,8] Evidence also suggests a role for iPLA$_2\beta$ in TAG metabolism. Increased adipogenesis was observed in bone marrow stromal cells in iPLA$_2\beta^{-/-}$ mice.[9] Cell culture studies with CHO-K1 cells have shown that TAG synthesis and formation of cytosolic lipid droplets required the activity of iPLA$_2\beta$ under conditions devoid of exogenous fatty acids.[10]

Working with the rat hepatoma cell line McA-RH7777, we have previously obtained *in vitro* evidence that the activity of iPLA$_2\beta$ was required for the assembly and secretion of TAG-rich $VLDL_1$.[11] Production of hepatic $VLDL_1$ is achieved through the recruitment of various lipid substrates (mainly TAG) by apolipoprotein (apo) B-100 within the secretory compartments including endoplasmic reticulum (ER) and Golgi apparatus.[2] Depending upon the availability of lipids, the resulting VLDL particles vary from small $VLDL_2$ (S_f 20-100) to large $VLDL_1$ ($S_f > 100$).[12] Each resulting $VLDL_1$ or $VLDL_2$ particle contains a single copy of apoB-100. In McA-RH7777 cells when the iPLA$_2\beta$ activity was inhibited using a chemical inhibitor bromoenol lactone (BEL) or antisense oligonucleotides, assembly and secretion of $VLDL_1$, but not $VLDL_2$, was attenuated.[11] Similar requirement of the iPLA$_2\beta$ activity for $VLDL_1$ production was also observed in experiments using primary hepatocytes isolated from mouse.[11] Mechanisms by which the assembly and secretion of $VLDL_1$ requires the iPLA$_2\beta$ activity remain undefined, nor is it known whether or not iPLA$_2\beta$ expression would play a role in lipoprotein production *in vivo*.

NAFLD, especially nonalcoholic steatohepatitis (NASH), are considered as a major risk factor for hepatocellular carcinoma (HCC).[13-16] In this regard, enhanced secretion of TAG as VLDL would be an effective cytoprotective mechanism in preventing NAFLD, NASH, and HCC. To gain an insight into the role of iPLA$_2\beta$ in hepatic TAG metabolism *in vivo*, we generated an iPLA$_2\beta$-null mouse model and examined the effect of global iPLA$_2\beta$ inactivation on TAG concentrations in the liver as well as plasma TAG-rich lipoproteins under chow and high-fat diet (HFD) conditions. The present data suggest that the loss of iPLA$_2\beta$ activity resulted in increased TAG-rich $VLDL_1$ production in cultured hepatocytes under lipid-rich conditions. However, the lack of iPLA$_2\beta$ gene expression does not appear to have an impact on liver or plasma TAG concentrations *in vivo*.

MATERIALS AND METHODS

1. Materials

Cell culture media and reagents were obtained from Invitrogen (Burlington, ON). [^{35}S]Methionine/cysteine (1,000 Ci/mmol) and [^{3}H]acetic acid (0.1 Ci/mmol) was obtained from PerkinElmer (Woodbridge, ON). [^{3}H]glycerol were obtained from American Radiolabeled Chemicals (St. Louis, MA). [^{3}H]Palmitic acid (54 Ci/mmol), protein A-sepharose CL-4B beads, horseradish peroxidase-linked anti-mouse and anti-rabbit IgG antibodies were obtained from GE Healthcare (Mississauga, ON). Horseradish peroxidase linked anti-goat antibody, fibronectin and collagenase were obtained from Sigma-Aldrich (Oakville, ON). Protease inhibitor cocktail and chemiluminescent substrates were obtained from Roche Diagnostics (Laval, PQ). Poloxamer 407 (P407) was a gift from BASF Corporation (Florham Park, NJ). Polyclonal antisera against apoA-I or apoE were obtained from BioDesign International (Saco, ME). Goat anti-apoB antibody was obtained from Millipore (Billerica, MA). Polyclonal antisera against rat VLDL (used for immunoprecipitation of apoB-100) were generated in our laboratory.

2. Construction of targeting vector and generation of iPLA$_2\beta$ knockout mice

The global iPLA$_2\beta$ knockout mice were achieved by replacing exon 2 of the *iPLA$_2\beta$* gene with a *neo* gene (see details in legend to Fig. 1A). The iPLA$_2\beta$ gene knockout was verified by PCR with mouse tail genomic DNA (Fig. 1B) and by RT-PCR with liver mRNA (Fig. 1C). The primers for generating the targeting vector and for animal screening were listed in supplemental Table S1. Male iPLA$_2\beta^{-/-}$ mice were infertile and some female iPLA$_2\beta^{-/-}$ mice were blind. Male iPLA$_2\beta^{+/-}$ were backcrossed with female iPLA$_2\beta^{-/-}$ mice for up to ten generations prior to experimentations.

3. The iPLA$_2\beta$ activity assay

Mouse livers were minced by Dounce homogenizer (20 strokes) in a buffer containing 20 mM Tris-HCl, pH 7.5, 0.25 M sucrose, 2 mM EDTA, 10 mM EGTA, 1 mM PMSF, 20 μM leupeptin, and 1 mM DTT. The cytosol was obtained by

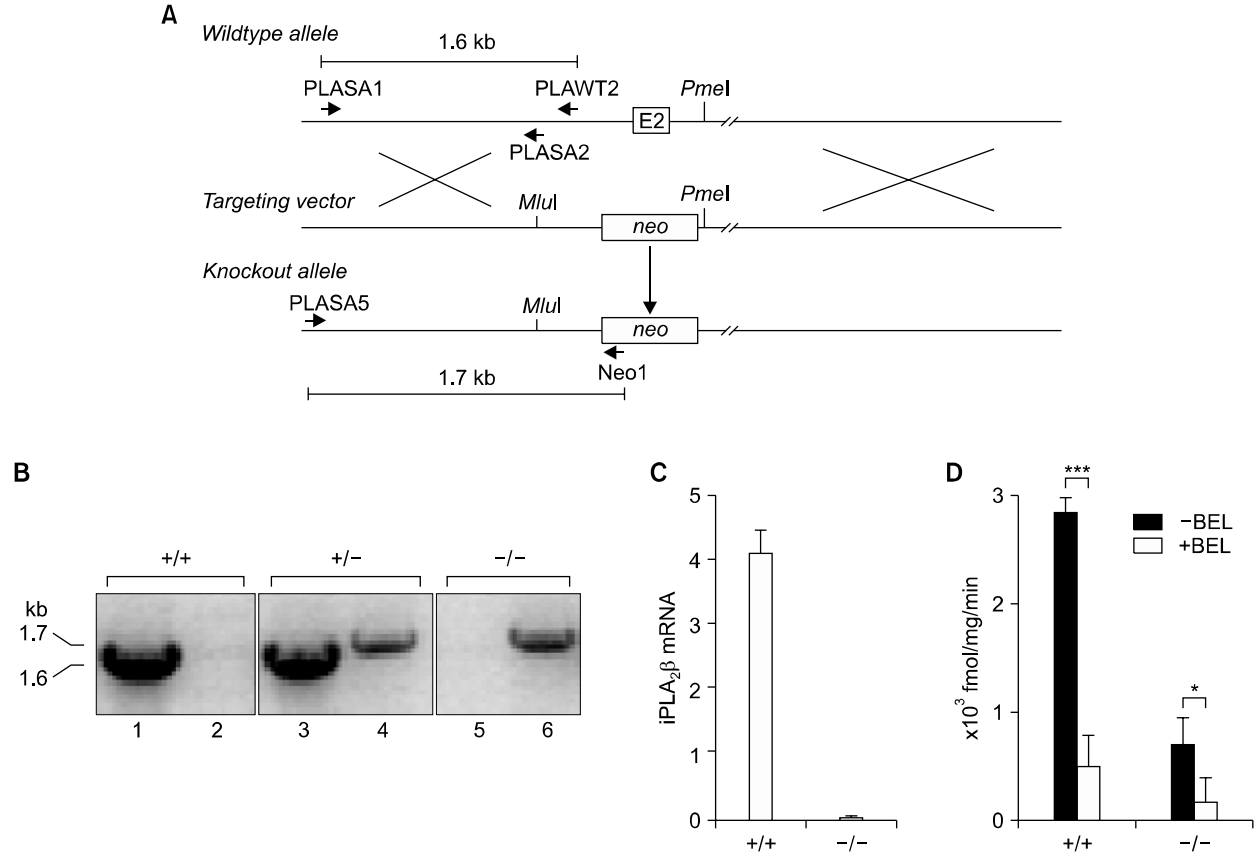

Fig. 1. Global inactivation of iPLA$_2\beta$ and characterization of iPLA$_2\beta^{-/-}$ mice. (A) Strategy for targeting the iPLA$_2\beta$ allele. In this strategy, 800 bp of sequence upstream and 440 bp of sequence downstream of ATG (translation start) in exon 2 (E2) were replaced by the *neo* gene cassette. The targeting vector was constructed by using a 1.5-kb DNA fragment as the short arm, which was a PCR fragment from PLASA1 (located 2.2 kb upstream of exon 2 (containing the ATG start codon)) to PLASA2 (located in 788 Kb upstream of exon 2). The short arm was inserted at 5'end of the *neo* gene cassette using a *Mlu*I site. The long arm was an 11-kb genomic fragment which started from *Pme*I site to the end of the lambda clone. The targeting vector was linearized and then transfected by electroporation into 129 SvEv iTL1 embryonic stem cells. The positive clones, obtained after G418 selection and PCR screening with primer PLASA5 (38 bp upstream of PLASA1) and NEO1 (located in the 5'-promoter region of the *neo* gene), were microinjected into C57BL/6J blastocysts to generate chimeric mice. Arrows indicate positions of the PCR primers. (B) Genotyping iPLA$_2\beta^{+/+}$, iPLA$_2\beta^{+/-}$ and iPLA$_2\beta^{-/-}$ mice by PCR with mice tail genomic DNA. The wild-type allele was verified by PCR using the primer pair PLASA1 and PLAWT2 (146 bp downstream of PLASA2) that yielded a 1.6-kb fragment (lanes 1, 3 and 5). The iPLA$_2\beta$ gene knockout was verified by RT-PCR using the PLASA5/NEO1 primer pair that gave rise to a 1.7-kb fragment (lanes 2, 4, and 6). (C) RT-PCR analysis of iPLA$_2\beta$ mRNA in the livers of iPLA$_2\beta^{+/+}$ and iPLA$_2\beta^{-/-}$ mice. (D) The iPLA$_2\beta$ activity in the liver cytosol of iPLA$_2\beta^{+/+}$ and iPLA$_2\beta^{-/-}$mice (n=3 for each group). The iPLA$_2\beta$ activity was determined in the presence (+*BEL*) or absence (−*BEL*) of bromoenol lactone. *P<0.05; ***P<0.001 (iPLA$_2\beta^{+/+}$ *versus* iPLA$_2\beta^{-/-}$).

centrifugation of the post-nuclear supernatant (100,000 rpm, 16 min, 4°C). The PLA_2 activity in the cytosol was measured using [^{3}H]palmitoyl-phosphatidylcholine as a substrate in the presence or absence of 10 mM $CaCl_2$. Dithiothreitol (0.5 mM) was present when PLA_2 activity was determined in the absence of $CaCl_2$.[17] In some assays, 90 μM BEL (Cayman Chemical, Ann Arbor, MI) was included in the assay mix (Fig. 1D).

4. Animals and diet

Mice were maintained and bred in a temperature-controlled facility with fixed 12 h light/dark cycles and free access to regular chow diet (Harlan, Teklad global 18% protein rodent diet 2018) and water. In some experiments mice were fed a HFD (Harlan, TD.88137-adjusted calories diet (42% from fat)) for an indicated period of time. All experiments were performed according to protocols approved by the Animal Studies Committee at the University of Ottawa.

5. Western blot analysis of apolipoproteins

Plasma samples were collected by saphenous vein bleeding from either chow or HFD fed mice treated with or without P407 (1 mg/g body weight; injected intraperitoneally). Equal volume of plasma sample was resolved by SDS-PAGE (5% or 10% gel), and apoB, apoE, and apoA-I were detected by Western blot analysis using appropriate antibodies. In some experiments, the plasma samples were pooled from 3-4 mice and fractionated by cumulative rate flotation ultracentrifugation[18] or FPLC as previously described.[19,20] An aliquot of each fraction (0.92 ml from ultracentrifugation and 0.5 ml from FPLC) was resolved by SDS-PAGE (5-15% gradient gel) to detect apoB, apoE, and apoA-I. Intensity of apoprotein bands was quantified by scanning densitometry using Quantity One software (Bio-Rad, Mississauga, ON).

6. Histology of tissue specimen

Liver and thigh skeletal muscle samples were cut into thin slices and stained with hematoxylin & eosin (H&E).[21] Thigh subcutaneous adipose tissues were frozen and then sectioned into thin slices followed by staining with Oil Red O.[22] The specimen sections were scanned using Zeiss Mirax Midi microscope scanner and the images were analyzed using Mirax Viewer software (Carl Zeiss Canada Ltd., Toronto).

7. Measurement of plasma and tissue lipids

Plasma samples were collected and fractionated as described above. Total TAG (Genzyme or Thermo Scientific), cholesterol (Wako, Richmond, VA), and phosphatidylcholine (Wako) were quantified using commercial assay kits according to manufacturers' instructions. For tissue TAG and cholesteryl ester (CE) mass measurement, lipids were extracted with Folch method[23] and samples were processed as previously described.[24] Liver, adipose tissue, and skeletal muscle samples (~100 mg) were homogenized with polytron (Kinematica AG, PT10-35) in $CHCl_3$: CH_3OH (2 : 1; v/v) and the homogenate was mixed overnight. Solvent phase was collected by centrifugation and the pellet was washed once with $CHCl_3$: CH_3OH (2 : 1; v/v). Combined organic solvent was dried under N_2 in 60°C water bath and resuspended in 6 ml of $CHCl_3$: CH_3OH (2 : 1; v/v) plus 1.2 ml of 0.05% H_2SO_4. Aqueous and organic solvent phases were separated by centrifugation, and 200 μl of organic phase was dried under N_2. Lipids were emulsified by mixing with 2 ml of 1% Triton X-100 (in $CHCl_3$), dried again, and dissolved in 1 ml of H_2O. TAG, PC, and CE were quantified as described above.[24]

8. Preparation of mouse primary hepatocytes

Mouse primary hepatocytes were isolated by a collagenase perfusion technique as described previously[25] with slight modifications. Mouse livers were first perfused with 50 ml of oxygenated Ca^{2+}/Mg^{2+}-free HEPES buffer I (0.15 M NaCl, 6.7 mM KCl, 10 mM HEPES, 0.5 mM EGTA, pH7.4), and then with 50 ml of collagenase (0.5 mg/ml) in oxygenated HEPES buffer II (67 mM NaCl, 6.7 mM KCl, 5 mM $CaCl_2$ and 100 mM HEPES, pH 7.6). After perfusion, the liver was excised, minced with scissors in William's medium E, and cells were dispersed with gentle shaking. The cell suspension was filtered through a cell strainer (BD Falcon, Bedford, MA), and washed twice with 30 ml of complete medium (William's medium E containing 10% FBS and 1% antibiotic-antimycotic). Cells were seeded onto fibronectin-coated 60 mm dishes (2×10^6 cells per

dish) and maintained at 37°C with 5% CO_2 for 2 h. The media were replaced with fresh complete media for another 2 h prior to experiments.

9. Pulse-chase and continuous labeling of apolipoproteins and lipids

In pulse-chase experiments, hepatocytes were labeled with [^{35}S]methionine/cysteine (100 μCi/ml) for 3 h in methionine/cysteine-free DMEM, and then chased with normal DMEM for up to 4 h. Both pulse and chase media were supplemented with 10% FBS and 0.4 mM oleic acid. In protein continuous labeling experiments, primary hepatocytes were labeled with [^{35}S]methionine/cysteine (100 μCi/ml) for 1.5 and 3 h in methionine/cysteine-free DMEM containing 10% FBS and 0.4 mM oleic acid. ApoB and apoE were recovered from cell and media, respectively, by immunoprecipitation using appropriate antibodies, resolved by SDS-PAGE and visualized by fluorography. Radioactivity associated with apoB and apoE were quantified by scintillation counting. In lipid continuous labeling experiments, primary hepatocytes (isolated from HFD-fed mice) were labeled with [^{3}H]acetic acid (10 μCi/ml) for up to 6 h in DMEM. Lipids were extracted from cell and media, respectively, resolved by TLC, and ^{3}H-PC and ^{3}H-TAG was quantified by scintillation counting.

RESULTS

1. Generation of global iPLA$_2\beta$ knockout mice in C57BL/6 mice

Inactivation of iPLA$_2\beta$ was achieved by disruption of exon 2 (containing the translation start codon ATG) using the *neo* gene cassette in 129 SvEv iTL1 embryonic stem cells (Fig. 1A). The positive stem cell clones were injected into C57BL/6J blastocytes to generate chimeric mice. The male iPLA$_2\beta^{+/-}$ mice were backcrossed with female iPLA$_2\beta^{-/-}$ mice for up to ten generations to achieve iPLA$_2\beta$-null in C57BL/6 background. Analysis of mice tail genomic DNA by RT-PCR confirmed the iPLA$_2\beta^{-/-}$ genotype (Fig. 1B). As noted before, male iPLA$_2\beta^{-/-}$ mice were infertile.[26] It was also noted that some female iPLA$_2\beta^{-/-}$ mice were blind. Thus in most subsequent experiments, male iPLA$_2\beta^{-/-}$ mice were used. Analysis of the iPLA$_2\beta$ expression by RT-PCR showed nearly absence of iPLA$_2\beta$ mRNA in the resulting iPLA$_2\beta^{-/-}$ mice liver homogenates (Fig. 1C). Enzymatic assay using liver homogenate showed that the BEL-sensitive iPLA$_2$ activity in iPLA$_2\beta^{-/-}$ liver was decreased to $<$25% of normal (Fig. 1D). The residual iPLA$_2$ activity in the iPLA$_2\beta^{-/-}$ liver might be contributed by other PLA2 enzymes.

Table 1. Lipid content of plasma collected from iPLA$_2\beta^{+/+}$ and iPLA$_2\beta^{-/-}$ mice under different age and diet conditions

Age (wk)	Sex	No. of mice	Diet	Fast (h)	TC*		PC*		TAG*	
					iPLA$_2\beta^{+/+}$	iPLA$_2\beta^{-/-}$	iPLA$_2\beta^{+/+}$	iPLA$_2\beta^{-/-}$	iPLA$_2\beta^{+/+}$	iPLA$_2\beta^{-/-}$
12	F	4	Chow	16	108±16	105±6	182±27	176±14	64±11	62±9
12	M	4	Chow	16	114±16	98±6	330±50	292±51	73±12	74±17
40	F	2	Chow	0	102±3	87±30	185±8	169±47	84±24	95±34
40	F	2	Chow	6	80±6	77±19	152±15	148±32	52±3	51±8
9	M	4	Chow	5	nd	nd	nd	nd	52±8	46±4
9	M	4	HFD (2 wk)	5	nd	nd	nd	nd	61±6	42±2
12	M	6	HFD (3 wk)	0	184±20	146±57	nd	nd	100±17	73±15
9	M	4	HFD (4 wk)	5	nd	nd	nd	nd	51±8	54±8
12	M	6	HFD (5 wk)	0	105±22	91±35	nd	nd	49±13	48±12
9	F	4	Chow	5	103±4	97±12	204±13	194±27	48±5	44±7
9	F	4	HFD (2 wk)	5	126±11	127±4	177±18	167±8	44±5	43±3
9	F	4	HFD (4 wk)	5	132±9	149±23	160±8	172±17	47±6	46±5
9	F	4	HFD (6 wk)	5	140±13	146±24	172±11	167±22	50±5	50±9
9	F	4	HFD (8 wk)	5	165±19	165±19	198±18	190±13	51±6	53±6

Plasma lipid measurements were determined from mice at indicated age that were maintained either in chow diet only or in chow diet followed by high fat diet (HFD) for indicated week followed by either fasting for indicated duration or postprandial (PP) (i.e. 0 h fasting) conditions. *mg/dl; nd, not determined.

2. Normal plasma lipid/lipoprotein concentrations and tissue lipid levels in iPLA$_2\beta^{-/-}$ mice

We determined fasting plasma TAG, total cholesterol (TC), and phospholipid (PC) concentration in 12 weeks old mice (female and male) under chow diet fed conditions, and did not detect noticeable changes in these lipids between iPLA$_2\beta^{+/+}$ and iPLA$_2\beta^{-/-}$ mice (Table 1, top two rows). We then determined the plasma lipids in 40 weeks old female mice (fed with chow diet) either under fasting or non-fasting (postprandial; PP) conditions, and did not detect any change in plasma lipids between iPLA$_2\beta^{+/+}$ and iPLA$_2\beta^{-/-}$ mice (Table 1, third and fourth rows). We then fed a group of male mice (9 or 12 weeks old) high-fat diet for 2, 3, 4, and 5 weeks. There was no change in the plasma TAG, TC, or PC between iPLA$_2\beta^{+/+}$ and iPLA$_2\beta^{-/-}$ mice (Table 1, fifth to ninth rows). Finally, we placed a group of female mice (9 weeks old) on high-fat diet for a period of 2, 4, 6, and 8 weeks, and determined fasting plasma lipids at the end of respective dieting. Again, there was no difference in plasma lipids between iPLA$_2\beta^{+/+}$ and iPLA$_2\beta^{-/-}$ mice (Table 1, bottom five rows).

We further fractionated plasma lipoproteins, by cumulative rate flotation ultracentrifugation, into VLDL$_1$, VLDL$_2$, intermediate density lipoprotein (IDL)/low density lipoprotein (LDL), and high density lipoprotein (HDL) fractions at the end of 8-week feeding, and analyzed TAG and TC distribution among the lipoproteins. Results shown in Fig. 2A indicated that TAG and TC distribution among the fractionated lipoproteins was nearly identical between iPLA$_2\beta^{+/+}$ and iPLA$_2\beta^{-/-}$ mice. Unchanged distribution of TAG or PC among plasma lipoproteins between the two groups of mice was also observed when plasma lipoproteins were fractionated using FPLC, instead of ultracentrifugation (results not shown).

To determine if iPLA$_2\beta$ inactivation has an impact on TAG production, we quantified TAG accumulation in the plasma after injection with P407 to block lipolysis of newly secreted VLDL. As shown in Fig. 2B, the rate of TAG accumulation in the plasma during a period of 2 h was nearly identical between iPLA$_2\beta^{+/+}$ and iPLA$_2\beta^{-/-}$ mice. Further quantification of the rate of TAG production showed no statistic difference between the two groups of mice (Fig. 2C). We further analyzed the TAG production by metabolic labeling using [^{3}H]glycerol (injected together with P407), and determined distribution of ^{3}H-TAG and ^{3}H-PC among fractionated lipoproteins. It was noted that although there was no difference in the rate of TAG mass production, the amount of metabolically labeled ^{3}H-TAG in VLDL$_1$ fractions was increased (by $>50\%$) in iPLA$_2\beta^{-/-}$ mice (Fig. 2D, left panel). The distribution of ^{3}H-PC among lipoproteins was unchanged between iPLA$_2\beta^{+/+}$ and iPLA$_2\beta^{-/-}$ mice (Fig. 2D, right panel). Taken together, these results suggested that iPLA$_2\beta^{-/-}$ mice are overall normolipidemic. Thus, global inactivation of iPLA$_2\beta$ did not result in changes in plasma TAG or TC mass, although the association of metabolically labeled TAG in VLDL$_1$ might be increased in iPLA$_2\beta^{-/-}$ mice.

3. Impact of inactivation of iPLA$_2\beta$ on plasma apolipoproteins

We determined the concentration of plasma apolipoproteins in iPLA$_2\beta^{+/+}$ and iPLA$_2\beta^{-/-}$ mice fed with chow diet. Semi-quantitative Western blot analysis showed that there was no detectable change in apoB-100, apoB-48, apoE, or apoA-I between the two groups of chow diet-fed mice, either in fasting or non-fasting plasma (results not shown). The lack of a difference in apoB-100, apoB-48, apoE, or apoA-I was observed regardless of age [i.e. young (12-14 weeks of age) versus old (40-44 weeks of age)] or sex (i.e. female versus male) (results not shown).

We next examined the effect of iPLA$_2\beta$ inactivation on plasma lipoprotein profiles in male mice fed HFD. Under this condition, semi-quantitative western blot analysis showed that there was a trend of increase in apoB-100 and apoB-48 in iPLA$_2\beta^{-/-}$ mice as compared with that in iPLA$_2\beta^{+/+}$ mice (Fig. 3A, top two panels). The concentrations of apoE or apoA-I in fasting plasma were similar between the HFD-fed iPLA$_2\beta^{+/+}$ and iPLA$_2\beta^{-/-}$ mice (Fig. 3A. bottom two panels) period Fractionation of the fasting plasma, pooled from four mice fed HFD, showed that the increased apoB-100 was mainly present in IDL/LDL fractions (Fig. 3B, top two panels).

To determine further whether or not iPLA$_2\beta$ inactivation had an effect on apoB production, we performed *in vivo* metabolic labeling using [^{35}S]methionine with mice fed

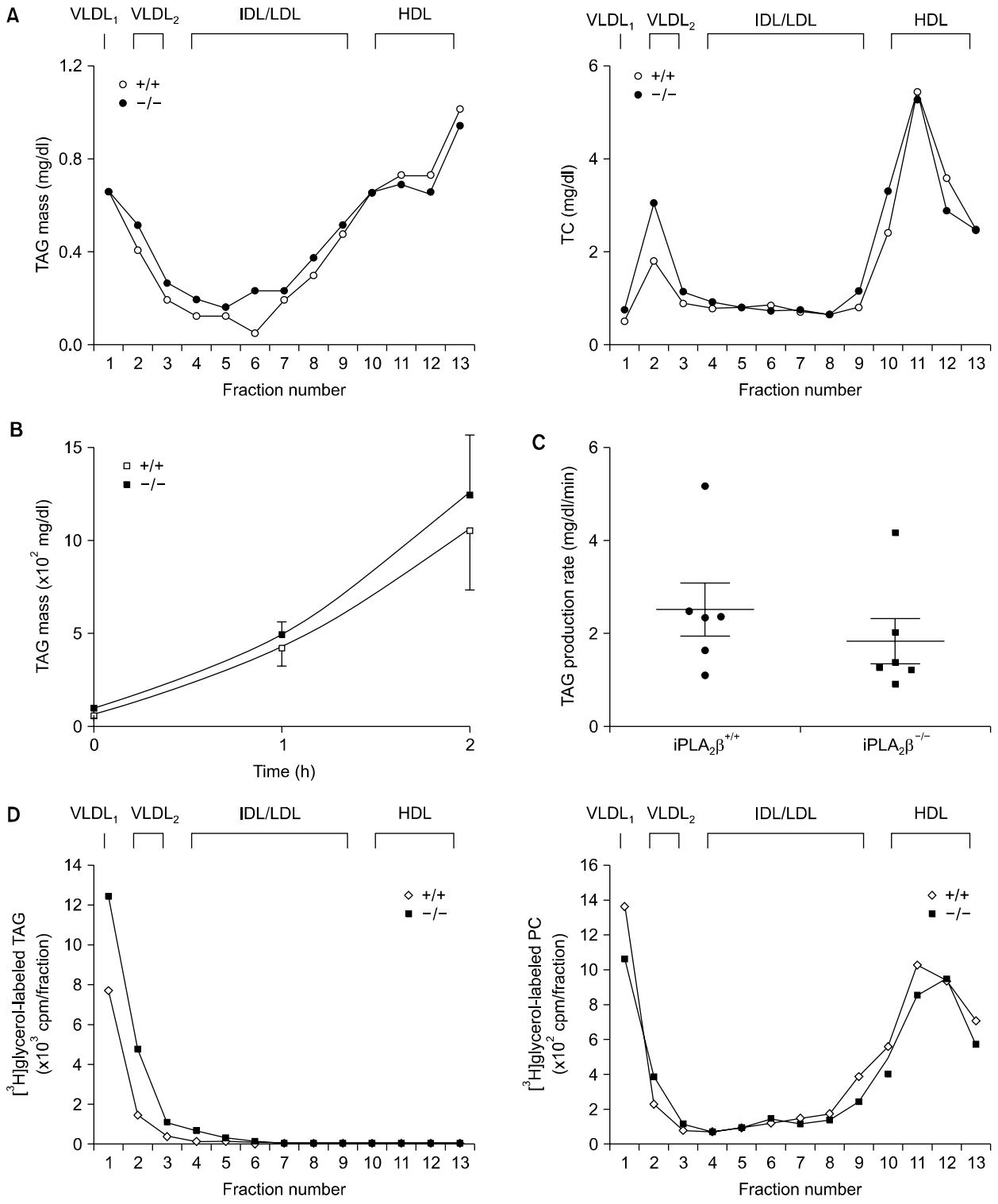

Fig. 2. TAG and cholesterol mass in iPLA$_2\beta^{-/-}$ and iPLA$_2\beta^{+/+}$ mice fed HFD. (A) Plasma samples from four mice (iPLA$_2\beta^{+/+}$ or iPLA$_2\beta^{-/-}$) fed HFD were pooled and fractionated by cumulative rate flotation ultracentrifugation. Lipids in each fraction were extracted, resolved by TLC, and the mass of TAG (left panel) and total cholesterol (TC) (right panel) was quantified. (B) Mice [iPLA$_2\beta^{+/+}$ (n=4); iPLA$_2\beta^{-/-}$ (n=3)] fed with HFD were fasted for 6 h, and injected with P407. Plasma was collected at 1 and 2 h after injection, pooled, and lipids were extracted. The lipids were resolved by TLC, and the TAG mass were quantified. (C) The experiment was performed the same as described in B, except that six mice from each group were used. The production rate of TAG is presented as mg/dl/min. (D) Mice [iPLA$_2\beta^{+/+}$ (n=4); iPLA$_2\beta^{-/-}$ (n=3)] fed with HFD for 2 weeks were fasted for 6 h, and injected with [^{3}H]glycerol (50 μCi) together with P407. Plasma was collected 2 h after injection, pooled, and fractionated into different lipoproteins. Lipids were extracted from each fraction, resolved by TLC. Radioactivity associated with ^{3}H-TAG (left panel) and ^{3}H-PC (right panel) were quantified by scintillation counting.

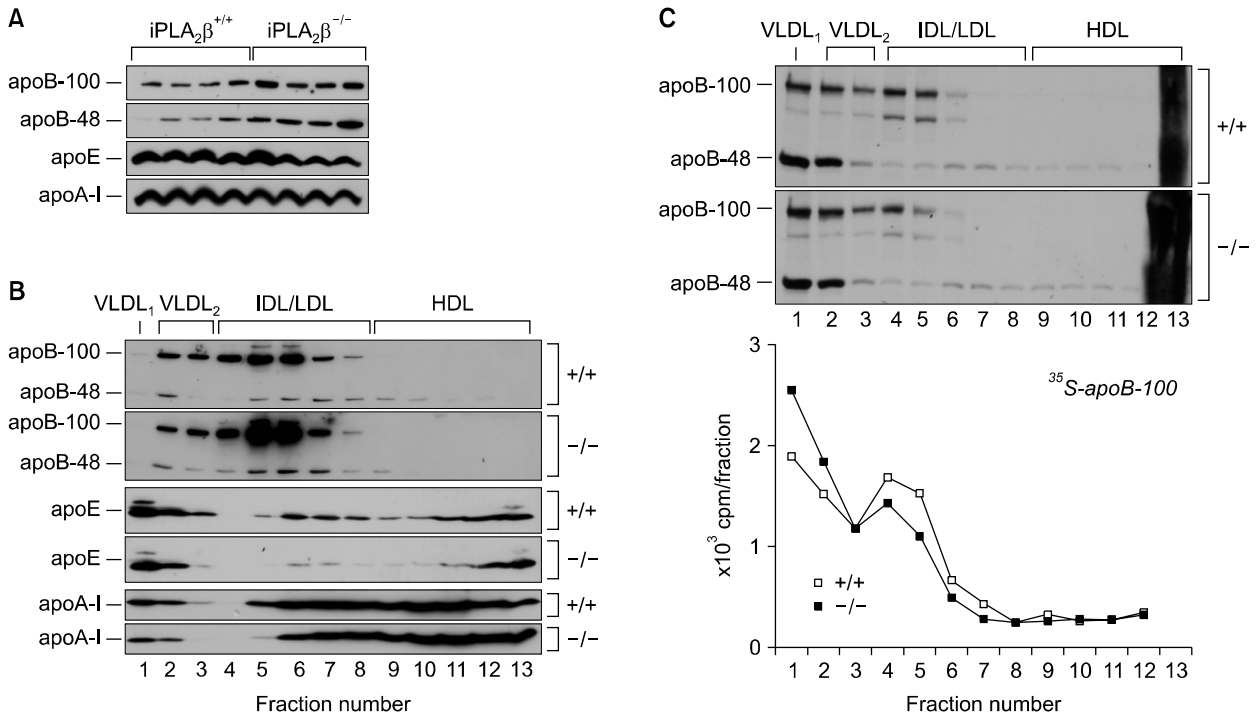

Fig. 3. Apolipoprotein concentrations in the plasma of $iPLA_2\beta^{-/-}$ and $iPLA_2^{+/+}$ mice fed HFD. (A) Plasma samples from four $iPLA_2\beta^{+/+}$ or $iPLA_2\beta^{-/-}$ mice were subjected to SDS-PAGE, and apoB-100, apoB-48, apoE, and apoA-I were detected by Western blot analysis using respective antibodies. (B) Plasma samples from four $iPLA_2\beta^{+/+}$ or $iPLA_2\beta^{-/-}$ mice were pooled and fractionated by cumulative rate flotation ultracentrifugation. ApoB-100, apoB-48, apoE, and apoA-I in each fraction was detected by Western blot analysis. (C) Mice [$iPLA_2\beta^{+/+}$ (n=4); $iPLA_2\beta^{-/-}$ (n=3)] fed with HFD for 2 weeks were fasted for 6 h, and injected with [^{35}S]methionine/cysteine (400 μCi) with P407. Plasma was collected 2 h after injection, pooled, and fractionated by cumulative rate flotation ultracentrifugation. ^{35}S-labeled apoB-100 and apoB-48 in each fraction were recovered by immunoprecipitation, resolved by SDS-PAGE, and visualized by fluorography (top panels). Radioactivity associated with ^{35}S-apoB-100 (bottom panel) and ^{35}S-apoB-48 (not shown) was quantified by scintillation counting. Results are presented as cpm per fraction.

HFD. The mice were injected with P407 prior to labeling. Fractionation of pooled plasma (2 h after injection) showed that there was an increase (by ~40%) in ^{35}S-apoB-100 in $VLDL_1$ fractions in $iPLA_2\beta^{-/-}$ plasma (Fig. 3C; top, representative fluorography; bottom, quantification of [^{35}S] radioactivity). The radioactivity associated with ^{35}S-apoB-48 was identical between $iPLA_2\beta^{+/+}$ and $iPLA_2\beta^{-/-}$ mice (results not shown). These data, in agreement with the metabolic labeling experiments for lipids (Fig. 2D), suggest that $iPLA_2\beta$ inactivation might have resulted in increased $VLDL_1$ (both TAG and apoB-100) production in mice fed HFD.

4. Primary hepatocytes of $iPLA_2\beta^{-/-}$ mice secrete increased VLDL

To ascertain that $iPLA_2\beta$ knockout results in increased hepatic VLDL secretion, we determined synthesis and secretion of metabolically labeled apoB and TAG using primary hepatocytes isolated from HFD-fed male $iPLA_2\beta^{-/-}$ and $iPLA_2\beta^{+/+}$ mice (10-12 weeks of age). Synthesis and secretion of apoB-100, determined by continuous labeling experiments with [^{35}S]amino acids, showed that incorporation of ^{35}S into cell-associated apoB-100 was increased (by 50% at the end of 3-h labeling) in $iPLA_2\beta^{-/-}$ cells as compared to that in $iPLA_2\beta^{+/+}$ cells (Fig. 4A, left panel). Secretion of ^{35}S-apoB-100 from $iPLA_2\beta^{-/-}$ cells was also increased (by 2-fold) at the end of 3-h labeling (Fig. 4A, right panel). In contrast, the incorporation of ^{35}S label into cell-associated (Fig. 4B, left panel) or secreted (Fig. 4B, right panel) apoE was unchanged between $iPLA_2\beta^{+/+}$ and $iPLA_2\beta^{-/-}$ cells. Thus, the increased incorporation of ^{35}S label into apoB-100 observed in $iPLA_2\beta^{-/-}$ cells was not a nonspecific phenomenon. Pulse-chase experiments showed that the secretion efficiency of ^{35}S-apoB-100 (Fig. 4C, left

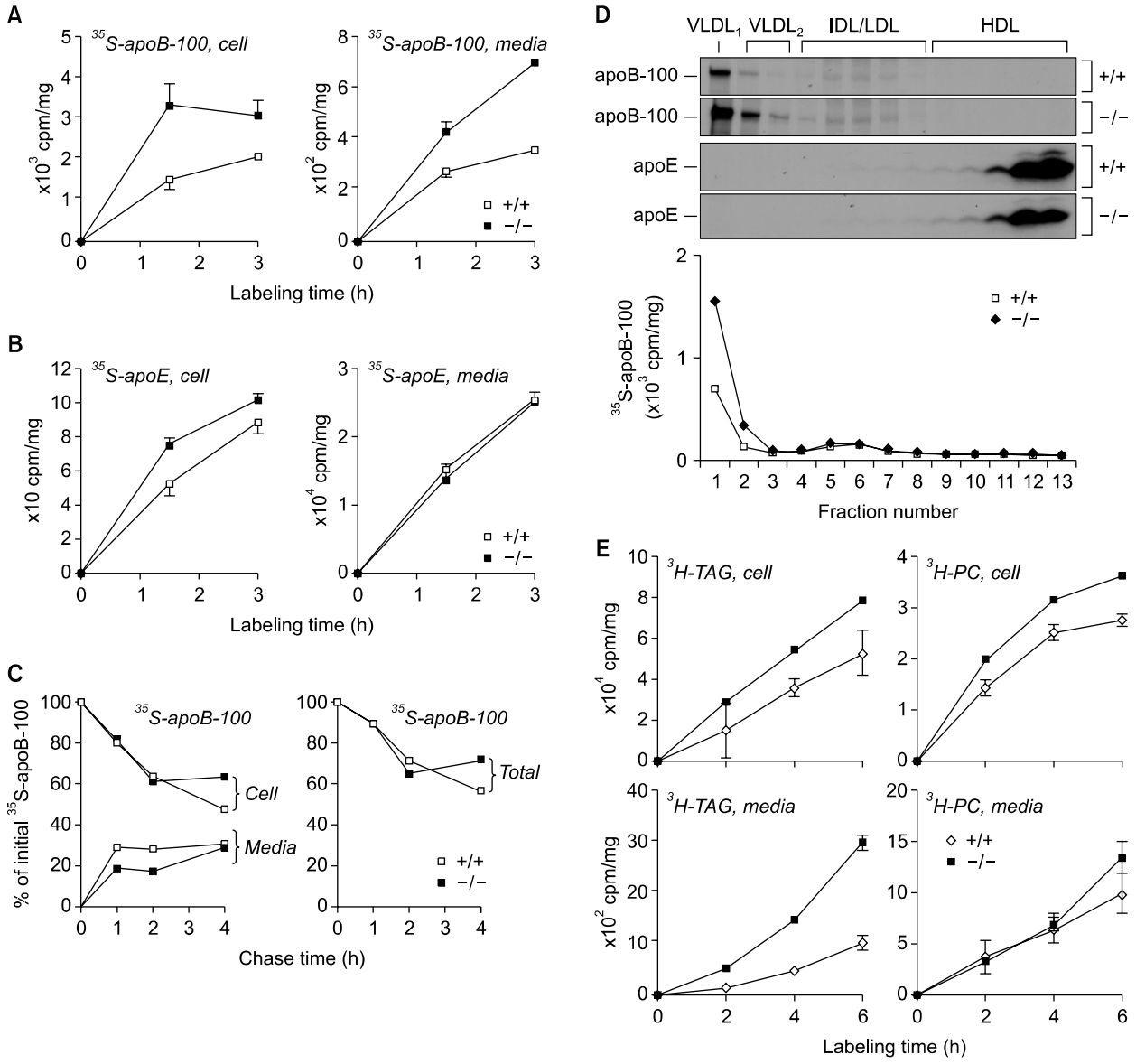

Fig. 4. Hepatocytes isolated from iPLA$_2\beta^{-/-}$ mice showed increased synthesis and secretion of ^{35}S-apoB-100 as VLDL$_1$. (A) Male mice (iPLA$_2\beta^{+/+}$ or iPLA$_2\beta^{-/-}$; 10 weeks old) were fed HFD for 2 weeks. Primary hepatocytes were isolated from these mice and labeled with [^{35}S]methionine/cysteine (100 μCi/ml) for 3 h in the presence of 10% FBS and 0.4 mM oleic acid. Incorporation of ^{35}S-label into cell-associated apoB-100 (left panels) and secreted apoB-100 in media (right panels) was quantified. (B) Incorporation of [^{35}S]label into cell-associated (left panels) and medium (right panels) apoE. (C) Pulse-chase analysis of apoB-100 secretion efficiency and post-translational stability. The hepatocytes were labeled for 3 h with [^{35}S]methionine/cysteine (100 μCi/ml), and chased for up to 4 h. Both pulse and chase media contained 10% FBS and 0.4 mM oleate. The ^{35}S-labeled apoB-100 was recovered from cells and media, respectively, by immunoprecipitation, and the radioactivity associated with ^{35}S-apoB-100 was quantified. Values at each chase time point are presented as percentage of initial cell-associated ^{35}S-apoB-100 (i.e. at the end of 3-h labeling). (D) Primary hepatocytes were labeled with [^{35}S]methionine/cysteine (100 μCi/ml) for 3 h in the presence of 10% FBS and 0.4 mM oleic acid. The conditioned media were fractionated by cumulate rate flotation ultracentrifugation. Radioactivity associated with apoB-100 and apoE was quantified. Data for ^{35}S-apoB-100 are presented as cpm/mg protein; data for ^{35}S-apoE are not shown. (E) Male mice were fed HFD for 19 days. Primary hepatocytes were labeled with [^{3}H]acetic acid (10 μCi/ml) for 2, 4 and 6 h. Lipids were extracted from cells and media, respectively, and resolved by TLC. Radioactivity associated with TAG and PC was quantified. Each value is the average of two dishes of cells (expressed as cpm/mg protein).

panel) was identical between iPLA$_2\beta^{+/+}$ and iPLA$_2\beta^{-/-}$ cells, and iPLA$_2\beta$ deficiency had no effect on total recovery of ^{35}S-apoB-100 during chase (Fig. 4C, right panel).

Fractionation of medium lipoproteins revealed that the increased ^{35}S-apoB100 secreted from iPLA$_2\beta^{-/-}$ cells was mainly associated with VLDL$_1$ (Fig. 4D, top two panels). Quantification of ^{35}S-apoB100 in fractionated lipoproteins confirmed that secretion of ^{35}S-apoB100 as VLDL$_1$ from iPLA$_2\beta^{-/-}$ cells was ~2-fold greater than that of iPLA$_2\beta^{+/+}$ cells (Fig. 4E). The amount of ^{35}S-apoE secreted from the

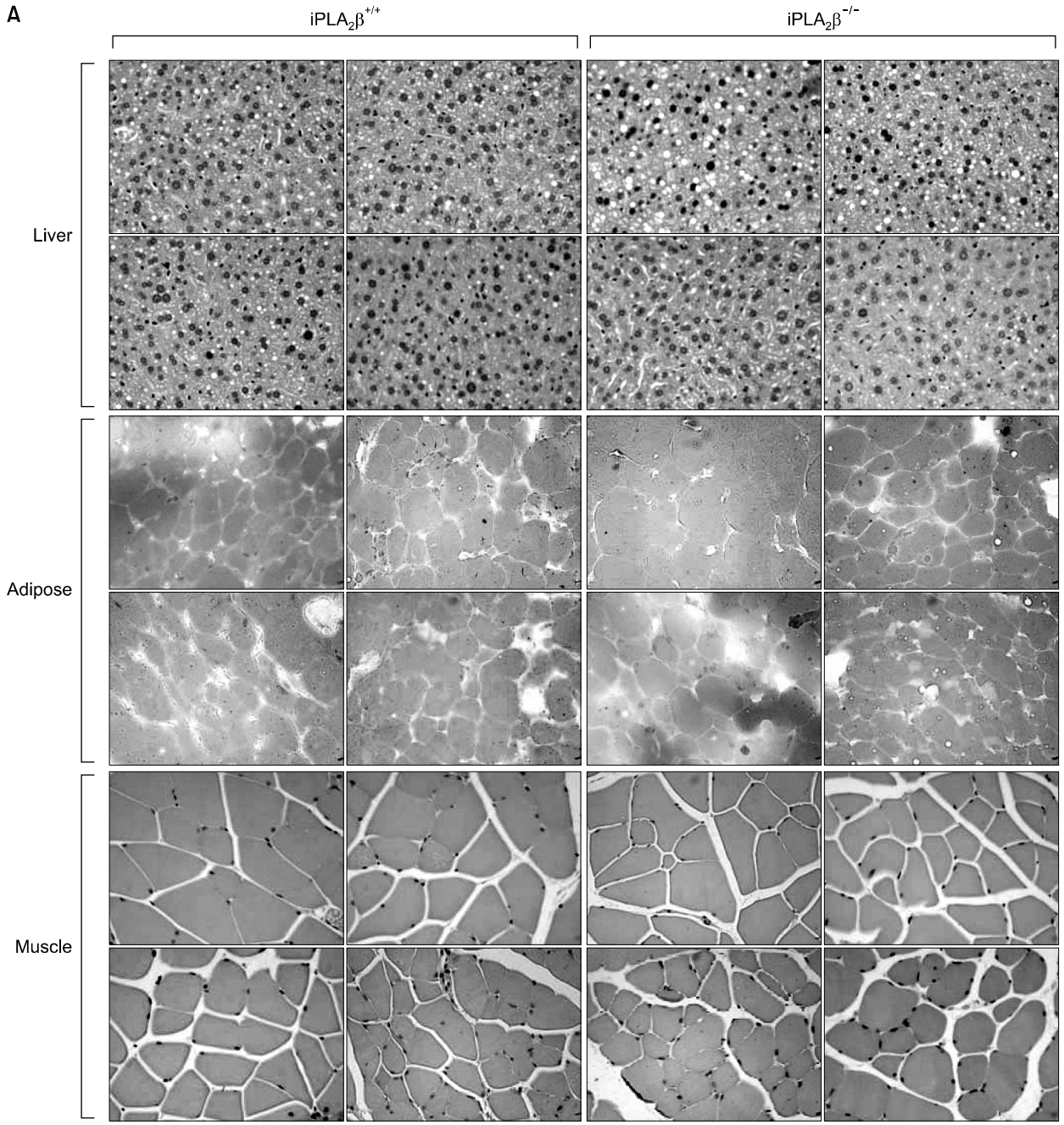

Fig. 5. Normal lipid mass in liver, adipose tissue, and skeletal muscle in iPLA$_2\beta^{-/-}$ mice. (A) Male iPLA$_2\beta^{+/+}$and iPLA$_2\beta^{-/-}$ mice (8–16 weeks of age) were fed HFD for 4 weeks. After 16 h fasting, the livers and thigh skeletal muscle were excised, processed and stained with H&E and the thigh adipose tissues were collected and stained with Oil Red O. Representative images are shown (400× magnification). (B) Lipids were extracted from respective tissues and quantified. Data are presented as mg/g tissue.

cells was associated mainly with HDL (Fig. 4D, bottom two panels). Quantification of ^{35}S label associated with apoE showed that secretion of ^{35}S-apoE was not changed between iPLA$_2\beta^{+/+}$ and iPLA$_2\beta^{-/-}$ cells (results not shown). These data suggest that secretion of apoB-100/VLDL$_1$ was specifically increased from cultured primary hepatocytes of iPLA$_2\beta^{-/-}$ mice.

We next determined whether or not iPLA$_2\beta^{-/-}$ inactivation resulted in changes in the expression of lipogenesis genes by quantitative RT-PCR analysis of mRNAs extracted from the liver (for RT-PCR primers please refer to Supplemental Table S2). However, we detected no differences in the mRNAs of genes involved in adipogenesis and TAG synthesis [e.g. *Srebf1* (SREBP1), *Dgat1* (DGAT1), *Dgat2* (DGAT2), Fasn (FAS) and *Gpam* (GPAT)], β-oxidation [e.g. *Ppara* (PPARα) and *Cpt1a* (CPT1)], VLDL production [e.g.

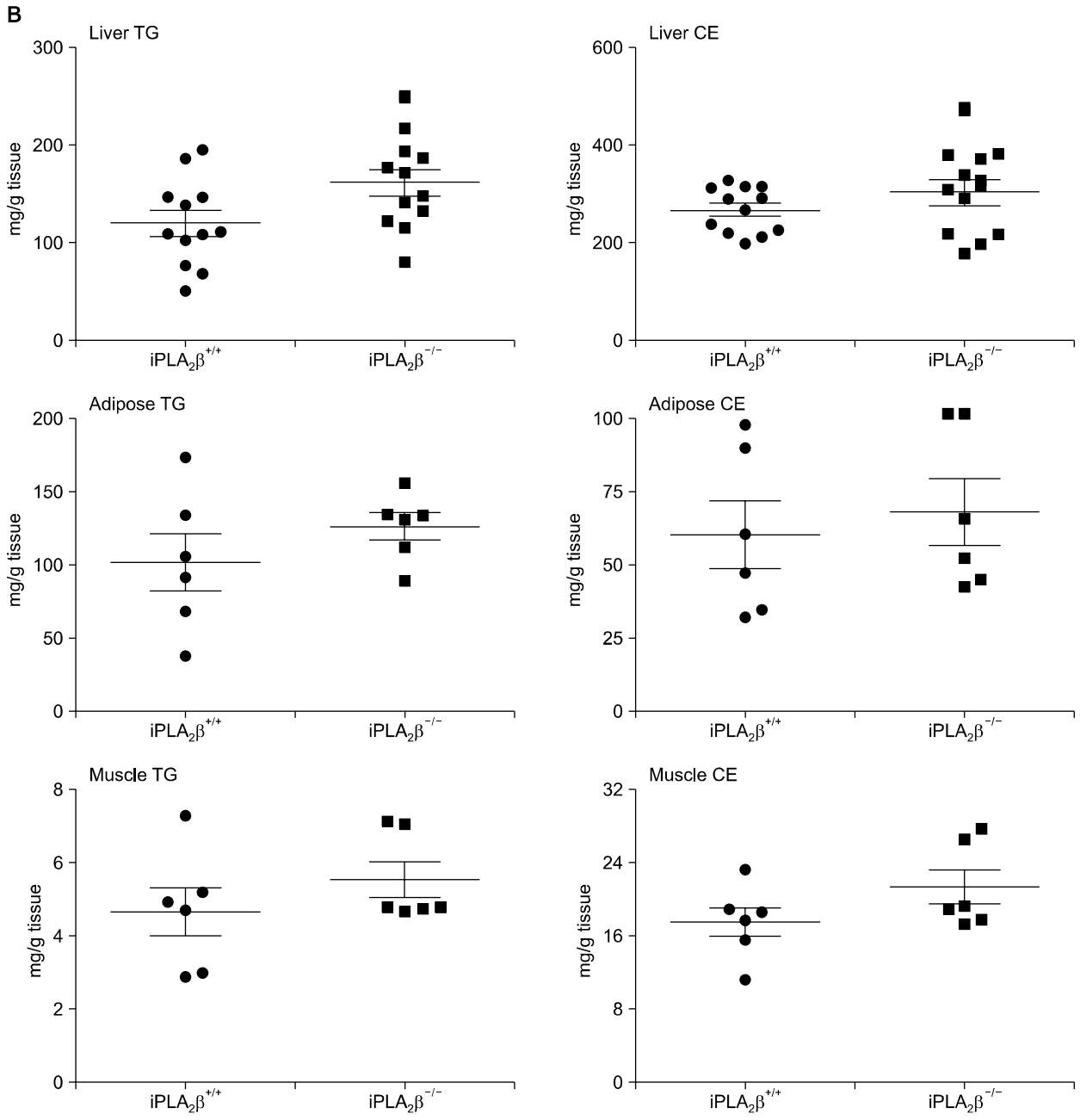

Fig. 5. Continued.

Apob (apoB), *Apoe* (ApoE) and *Mttp* (MTP)], or phospholipid synthesis [e.g. *Pemt* (phosphatidylethanolamine methyltransferase), *Pcyt1 α* (CTP: phosphocholine cytidylyltransferase), and *Pla2g4* (cPLA2)] (results not shown).

We then determined whether or not the lipogenesis was enhanced by metabolically labeling primary hepatocytes using [^{3}H]acetic acid. Incorporation of ^{3}H label into cell-associated PC and TAG was increased by 40% and 55%, respectively, in iPLA$_2\beta^{-/-}$ cells as compared to iPLA$_2\beta^{+/+}$ cells (Fig. 4E, top panels). Secretion of ^{3}H-TAG, but not ^{3}H-PC, from iPLA$_2\beta^{-/-}$ hepatocytes cells was increased as compared with iPLA$_2\beta^{+/+}$ cells (Fig. 4E, bottom panels). In a separate experiments, labeling the cells with [^{3}H]palmitic acid for 1 h also showed a trend of increased TAG synthesis in iPLA$_2\beta^{-/-}$ cells ($17.3\pm0.2\times10^4$ cpm/mg in iPLA$_2\beta^{+/+}$ cells, $20.1\pm1.1\times10^4$ cpm/mg in iPLA$_2\beta^{-/-}$ cells). Incorporation of [^{3}H]palmitic acid into PC was comparable between the two groups ($15.3\pm0.3\times10^4$ cpm/mg in iPLA$_2\beta^{+/+}$ cells, $14.0\pm1.1\times10^4$ cpm/mg in iPLA$_2\beta^{-/-}$ cells).

Additional pulse-chase experiments were performed to determine secretion efficiency of newly synthesized ^{3}H-TAG. In these experiments, primary hepatocytes were pulse-labeled with [^{3}H]palmitic acid for 1 h, and then chased in media supplemented with palmitic acid for up to 4 h. A 2-fold increase in the secretion of newly synthesized ^{3}H-TAG, but not ^{3}H-PC, occurred in iPLA$_2\beta^{-/-}$ hepatocytes as compared with iPLA$_2\beta^{+/+}$ cells (results not shown). These data suggest that iPLA$_2\beta$ inactivation might have resulted in increased lipogenesis/adipogenesis, which in turn resulted in increased secretion of newly synthesized TAG.

Finally, we determined whether or not increased lipogenesis would result in increased steatosis in the liver or peripheral tissues. To this end, we performed histological studies with the liver, thigh subcutaneous adipose tissue, and skeletal muscle (Fig. 5A) of male HFD mice, and quantified TG and CE in the respective tissues (Fig. 5B). There were no gross changes in the morphology in any of these tissues examined, nor were there significant changes in cellular TAG or cholesteryl ester concentrations between the iPLA$_2\beta^{+/+}$ and iPLA$_2\beta^{-/-}$ tissue samples, although there was a general trend of high TAG and CE in the tissues in iPLA$_2\beta^{-/-}$ mice.

DISCUSSION

In the present studies, we have determined the effect of global iPLA$_2\beta$ deficiency in C57BL/6 mice on TAG homeostasis *in vivo*. Results obtained from the current work suggest that the iPLA$_2^{-/-}$ mice displayed no discernible impact on total plasma lipids (e.g. TAG, CE and PC) or lipoproteins in mice fed either chow diet or HFD, and the lack of difference was observed in both female and male mice as well as in both young and old mice. Global iPLA$_2\beta$ deficiency also exerts no significant effect on the lipid mass in tissues examined, including liver, subcutaneous adipocytes, or skeletal muscles, although there might be a trend of high lipid mass in these tissues. However, because of the high inter-individual variation in iPLA$_2\beta^{-/-}$ as well as in iPLA$_2\beta^{+/+}$ mice, this trend of increase in tissue lipid mass does not reach statistical significance (Fig. 5). Thus, global iPLA$_2\beta$ inactivation in mice does not cause overt dyslipidemia.

However, metabolic labeling experiments, both *in vivo* (using P407 to block lipolysis) and *ex vivo* (using cultured primary hepatocytes) in conjunction with lipoprotein fractionation showed that iPLA$_2\beta$ deficiency was associated with increased secretion of VLDL apoB-100 and TAG. It is noteworthy that this increased hepatic secretion of VLDL from hepatocytes does not lead to hypertriglyceridemia in iPLA$_2\beta^{-/-}$ mice, which might be attributable to active catabolism of plasma VLDL.

An important observation of the present study was that both mass and metabolically labeled apoB-100 secretion was increased in iPLA$_2\beta^{-/-}$ mice, suggesting an increased VLDL$_1$ production under lipid-rich conditions. The high VLDL$_1$ secretion from the iPLA$_2\beta^{-/-}$ hepatocytes was associated with increased metabolic labeling of newly synthesized apoB-100 and TAG (Fig. 4), although there were no changes in mRNAs in any of the lipogenesis or VLDL synthesis genes examined (results not shown). Preliminary molecular species analysis of PC, phosphatidylethanolamine, and phosphatidylserine using tandem mass spectrometry also did not reveal discernible changes between iPLA$_2\beta^{-/-}$ and iPLA$_2\beta^{+/+}$ livers (results not shown), which are in agreement with data reported by other groups.[27] At the present we do not have a reasonable

explanation for the increased efficiency of hepatic VLDL assembly/secretion in iPLA$_2\beta^{-/-}$ mice. Our previous cell culture studies with McA-RH7777 cells showed that acute inhibition of iPLA$_2\beta$ (treated with BEL or antisense oligonucleotides) resulted in decreased secretion of TAG-rich lipoproteins without affecting TAG synthesis.[11] These data combined indicate that the acute and chronic iPLA$_2\beta$ deficiency exerted different effect on hepatic VLDL$_1$ assembly/secretion. In the global iPLA$_2\beta$ knockout mice, expression of other gene products might have altered that lead to increased VLDL production. The mechanisms by which hepatic VLDL secretion is increased upon iPLA$_2\beta$ inactivation in mice remain to be determined. Nevertheless, regardless of the mechanisms, enhanced VLDL production in iPLA$_2\beta^{-/-}$ mice does not lead to hyperlipidemia. The lack of changes in plasma lipoprotein concentration *in vivo*, in the face of increased VLDL production, may be attributable to altered catabolism of TAG-rich lipoproteins in iPLA$_2\beta^{-/-}$ mice. The possibility that TAG-rich lipoprotein catabolism is altered upon iPLA$_2\beta$ inactivation in mice also merits further investigation.

In summary, global inactivation of iPLA$_2\beta$ results in an enhanced hepatic VLDL secretion under high fat diet conditions with no symptoms of dyslipidemia in mice. The activity of iPLA$_2\beta$ could be a potential therapeutic target for preventing and treatment of diet-induced NAFLD and associated HCC complications.

ACKNOWLEDGEMENTS

The authors thank Dr Fengcheng Sun, Dr Maroun Bou Khalil, Dr Yuwei Wang, Dr. Michelle Bamji-Mirza, Sanjay Manhas, Erik F. Yao, Vincent Ngo, Yang Zhao, and Zheng Cui for technical assistance. This work is supported by a China-Canada Health Research Initiative Grant (CCI 92211) and an Operating Grant (NMD 15486) from Canadian Institute for Health Research.

SUPPLEMENTARY MATERIALS

Supplementary data including two tables can be found with this article online at http://pdf.medrang.co.kr/Jkacp/018/JCP13-013-s001.pdf.

REFERENCES

1. Johansen CT, Kathiresan S, Hegele RA. Genetic determinants of plasma triglycerides. J Lipid Res 2011;52:189-206.
2. Sundaram M, Yao Z. Recent progress in understanding protein and lipid factors affecting hepatic VLDL assembly and secretion. Nutr Metab (Lond) 2010;7:35-51.
3. Jiang ZG, Robson SC, Yao Z. Lipoprotein metabolism in nonalcoholic fatty liver disease. J Biomed Res 2013;27:1-13.
4. Teslovich TM, Musunuru K, Smith AV, Edmondson AC, Stylianou IM, Koseki M, et al. Biological, clinical and population relevance of 95 loci for blood lipids. Nature 2010;466:707-13.
5. Wilson PA, Gardner SD, Lambie NM, Commans SA, Crowther DJ. Characterization of the human patatin-like phospholipase family. J Lipid Res 2006;47:1940-9.
6. Jenkins CM, Yan W, Mancuso DJ, Gross RW. Highly selective hydrolysis of fatty acyl-CoAs by calcium-independent phospholipase A2beta. Enzyme autoacylation and acyl-CoA-mediated reversal of calmodulin inhibition of phospholipase A2 activity. J Biol Chem 2006;281:15615-24.
7. Balsinde J, Balboa MA. Cellular regulation and proposed biological functions of group VIA calcium-independent phospholipase A2 in activated cells. Cell Signal 2005;17:1052-62.
8. Ma Z, Turk J. The molecular biology of the group VIA Ca^{2+}-independent phospholipase A2. Prog Nucleic Acid Res Mol Biol 2001;67:1-33.
9. Ramanadham S, Yarasheski KE, Silva MJ, Wohltmann M, Novack DV, Christiansen B, et al. Age-related changes in bone morphology are accelerated in group VIA phospholipase A2 (iPLA2beta)-null mice. Am J Pathol 2008;172:868-81.
10. Gubern A, Barcelo-Torns M, Casas J, Barneda D, Masgrau R, Picatoste F, et al. Lipid droplet biogenesis induced by stress involves triacylglycerol synthesis that depends on group VIA phospholipase A2. J Biol Chem 2009;284:5697-708.
11. Tran K, Wang Y, DeLong CJ, Cui Z, Yao Z. The assembly of very low density lipoproteins in rat hepatoma McA-RH7777 cells is inhibited by phospholipase A2 antagonists. J Biol Chem 2000;275:25023-30.
12. Wang Y, Tran K, Yao Z. The activity of microsomal triglyceride transfer protein is essential for accumulation of triglyceride within microsomes in McA-RH7777 cells. A unified model for the assembly of very low density lipoproteins. J Biol Chem 1999;274:27793-800.
13. Duan XY, Qiao L, Fan JG. Clinical features of nonalcoholic fatty liver disease-associated hepatocellular carcinoma. Hepatobiliary Pancreat Dis Int 2012;11:18-27.
14. Ertle J, Dechene A, Sowa JP, Penndorf V, Herzer K, Kaiser G, et al. Non-alcoholic fatty liver disease progresses to hepatocellular carcinoma in the absence of apparent cirrhosis. Int J Cancer 2011;128:2436-43.
15. Jain D, Nayak NC, Kumaran V, Saigal S. Steatohepatitic hepatocellular carcinoma, a morphologic indicator of associated metabolic risk factors: a study from India. Arch Pathol Lab Med 2013;137:961-6.
16. Yu J, Shen J, Sun TT, Zhang X, Wong N. Obesity, insulin resistance, NASH and hepatocellular carcinoma. Semin

Cancer Biol 2013 (In Press).
17. Ackermann EJ, Conde-Frieboes K, Dennis EA. Inhibition of macrophage Ca^{2+}-independent phospholipase A2 by bromoenol lactone and trifluoromethyl ketones. J Biol Chem 1995; 270:445-50.
18. Redgrave TG, Carlson LA. Changes in plasma very low density and low density lipoprotein content, composition, and size after a fatty meal in normo- and hypertriglyceridemic man. J Lipid Res 1979;20:217-29.
19. Qin W, Sundaram M, Wang Y, Zhou H, Zhong S, Chang C-C, et al. Missense mutation in APOC3 within the C-terminal lipid-binding domain of human apoC-III results in impaired assembly and secretion of triacylglycerol-rich very low density lipoproteins. Evidence that apoC-III plays a major role in the formation of lipid precursors within the microsomal lumen. J Biol Chem 2011;286:27769-80.
20. Wang Y, McLeod RS, Yao Z. Normal activity of microsomal triglyceride transfer protein is required for the oleate-induced secretion of very low density lipoproteins containing apolipoprotein B from McA-RH7777 cells. J Biol Chem 1997;272:12272-8.
21. Cho SW, Kim SS, Rhie JW, Cho HM, Choi CY, Kim BS. Engineering of volume-stable adipose tissues. Biomaterials 2005;26:3577-85.
22. Cho SW, Kim SS, Rhie JW, Cho HM, Choi CY, Kim BS. Engineering of volume-stable adipose tissues. Biomaterials 2005;26:3577-85.
23. Folch J, Lees M, Sloane Stanley GH. A simple method for the isolation and purification of total lipides from animal tissues. J Biol Chem 1957;226:497-509.
24. Carr TP, Andresen CJ, Rudel LL. Enzymatic determination of triglyceride, free cholesterol, and total cholesterol in tissue lipid extracts. Clin Biochem 1993;26:39-42.
25. Yao ZM, Vance DE. The active synthesis of phosphatidylcholine is required for very low density lipoprotein secretion from rat hepatocytes. J Biol Chem 1988;263:2998-3004.
26. Bao S, Miller DJ, Ma Z, Wohltmann M, Eng G, Ramanadham S, et al. Male mice that do not express group VIA phospholipase A2 produce spermatozoa with impaired motility and have greatly reduced fertility. J Biol Chem 2004; 279:38194-200.
27. Bao S, Song H, Wohltmann M, Ramanadham S, Jin W, Bohrer A, et al. Insulin secretory responses and phospholipid composition of pancreatic islets from mice that do not express Group VIA phospholipase A2 and effects of metabolic stress on glucose homeostasis. J Biol Chem 2006;281: 20958-73.